

PAPER • OPEN ACCESS

Numerical analysis of double-layered microchannel heat sinks with different microchannel heights

To cite this article: S Savino and C Nonino 2020 *J. Phys.: Conf. Ser.* **1599** 012020

View the [article online](#) for updates and enhancements.



IOP | ebooks™

Bringing together innovative digital publishing with leading authors from the global scientific community.

Start exploring the collection—download the first chapter of every title for free.

Numerical analysis of double-layered microchannel heat sinks with different microchannel heights

S Savino and C Nonino

Università degli Studi di Udine, Dipartimento Politecnico di Ingegneria e Architettura,
Via delle Scienze 206, 33100 Udine

E-mail: stefano.savino@uniud.it

Abstract. A numerical parametric analysis is carried out to investigate the thermal performance of double-layered microchannel heat sinks for different values of the relative channel height and fixed values of the total pumping power, with the additional constraint that the pressure drop be the same in the two layers in order to allow a much simpler header design, which can only include a single inlet and a single outlet. Single-layered microchannel heat sinks are also considered for additional comparisons. The computed results show that, in the hypothesis of this work (i) the ratio of the heights of the upper and lower microchannels only has a marginal effect on the overall thermal resistance but a significant influence on the temperature uniformity of the bottom (heated) surface and (ii) a better temperature uniformity is achieved when the heights of the upper microchannels are larger than those of the lower ones.

1. Introduction

The continuous development of electronic technology leads toward higher and higher degrees of integration of electronic components on a single microchip which, in turn, implies a continuous increase of the heat generated per unit volume of the electronic components. The resulting need to dissipate always increasing heat fluxes can be very challenging, thus requiring the adoption of sophisticated cooling techniques. Among these, microchannel cooling, implemented in single or multi-layered heat sinks, is receiving increasing attention from researchers. Thus, in the last few years, several papers have been published on the subject [1–5]. In particular, it appears that the use of double-layered microchannel heat sinks (DL-MCHS), as an alternative to the more basic single layer arrangement, can offer some advantages in terms of reduction of the total thermal resistance, hotspot mitigation and temperature uniformity of the bottom wall of the heat sink, which is attached to the microchip [6, 7]. Recently some studies have been carried out to find optimal configurations of counter-flow DL-MCHS in terms of relative channel heights, lengths and liquid coolant velocities [8–12]. In nearly all cases, however, the optimization was carried out with reference to fixed values of the total pumping power without any other constraints, thus allowing the selection of average microchannel velocities that can lead to different values of the pressure drop in the two layers. While in principle this is feasible, it definitely represents a complication from a technical point of view since it implies that two micro-pumps and two separate pipelines are needed to carry the coolant.

In this paper, a numerical parametric analysis is carried out to investigate the thermal performance of DL-MCHS for different values of the relative channel height and fixed values of the total pumping power, with the additional constraint that the pressure drop be the same



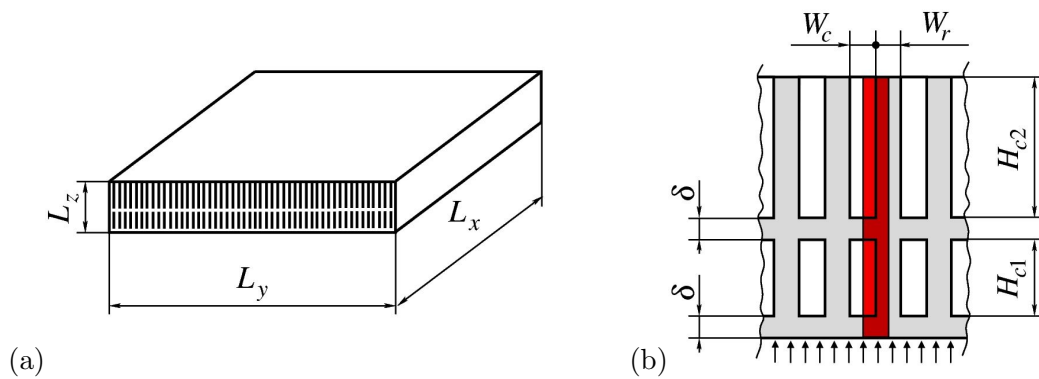


Figure 1. DL-MCHS: (a) 3-D sketch; (b) cross-section of a repetitive part of the geometry (shown in red) corresponding to the computational domain.

in the two layers in order to allow a much simpler header design, that can only include a single inlet and a single outlet. Single-layered MCHS are also considered for additional comparisons.

2. Statement of the problem and solution strategy

The basic DL-MCHS dimensions considered by Leng *et al.* [11] are also used in this parametric study, which concerns the thermal performance of two series of DL-MCHS, both having a footprint area of $L_x \times L_y = 10 \times 10 \text{ mm}^2$ and a total thickness of $L_z = 1.2 \text{ mm}$. A uniform heat flux $q''_w = 100 \text{ W/cm}^2$ is applied on the bottom wall of the heat sink, which is made of silicon. Water is the cooling fluid and flows in the two layers in counter-flow directions. As illustrated in Fig. 1, where a sketch of a DL-MCHS is reported together with the cross-section of a repetitive part of the geometry, W_c is the width of all microchannels, H_{c1} and H_{c2} are the heights of the lower and of the upper layer, respectively, while W_r is the width of all vertical ribs and $\delta = 100 \mu\text{m}$ is the thickness of all horizontal ones. The DL-MCHS of the two series differ for the number of microchannels N_m in each layer which are equal to those that, according to Leng *et al.* [11], with appropriate operating conditions and microchannel heights allow to achieve either a maximum temperature uniformity (series #1, $N_m = 54$) or a minimum total thermal resistance (series #2, $N_m = 64$) when the total pumping power Ω is equal to 0.05 W. The pumping power can be computed as

$$\Omega = N_m W_c (u_{c1} H_{c1} \Delta p_{c1} + u_{c2} H_{c2} \Delta p_{c2}) \quad (1)$$

where u_{c1} and u_{c2} are the average velocities in the microchannels of the lower and upper layers and Δp_{c1} and Δp_{c2} are the corresponding pressure drops. The maximum temperature uniformity is assumed to correspond to the minimum of the maximum temperature difference $\Delta T_{w,max} = T_{w,max} - T_{w,min}$, where $T_{w,max}$ and $T_{w,min}$ are the maximum and minimum temperatures on the bottom wall, i.e., that to be cooled, while, according to Leng *et al.* [11] and Wei *et al.* [6], the overall thermal resistance R_T is defined as

$$R_T = \frac{T_{w,max} - T_{in}}{Q} \quad (2)$$

where T_{in} is the uniform fluid inlet temperature and $Q = q''_w L_x L_y$ is the total heat load on the bottom wall. The values of the geometrical parameters and of the microchannel velocities u_{c1} and u_{c2} in the lower and upper layers identified by Leng *et al.* [11] for the two optimal conditions are reported in Table 1.

It must be pointed out that the listed combinations of microchannel heights and velocities yield different values of the pressure drop in the microchannels of the upper and lower layers

Table 1. Microchannel dimensions and velocities for minimum $\Delta T_{w,max}$ or minimum R_T and $\Omega = 0.05$ W according to Leng *et al.* [11].

Criterion	N_m	W_r [μm]	W_c [μm]	H_{c1} [μm]	H_{c2} [μm]	H_{c2}/H_{c1}	u_{c1} [m/s]	u_{c2} [m/s]
min $\Delta T_{w,max}$	54	95	88	141	859	6.09	0.99	0.78
min R_T	64	68	87	321	679	2.12	1.03	0.59

($\Delta p_{c1} \neq \Delta p_{c2}$), which implies that two micro-pumps and two separate pipelines are needed to carry the coolant. Even if this is feasible, it definitely represents a complication from a technical point of view, thus making the adoption of a DL-MCHS a less attractive solution for thermal control of micro chips. Therefore, it seems reasonable to investigate the performance of a DL-MCHS when the pressure drop is forced to be the same in both layers ($\Delta p_{c1} = \Delta p_{c2}$) since this would be the condition when only one micro-pump is used to circulate the coolant. To this purpose, with reference to the same values of N_m , W_r and W_c corresponding to the two optimal configurations identified by Leng *et al.* [11] for the minimization of $\Delta T_{w,max}$ or R_T with $\Omega = 0.05$ W, a parametric analysis is carried out where the values of the ratios H_{c2}/H_{c1} are varied while keeping the total height of the flow passages $H_{c1} + H_{c2}$ constant and equal to 1 mm. For the sake of completeness, single-layered microchannel heat sinks, which correspond to $H_{c2}/H_{c1} = 0$, are also considered. Three values of the total pumping power are assumed, namely, $\Omega = 0.0125$ W, 0.05 W and 0.20 W, while combinations of velocities u_{c1} and u_{c2} are imposed so that they yield the same pressure drop in the microchannels of the upper and lower layers in each DL-MCHS. The velocities u_{c1} and u_{c2} that produce the same pressure drop in both microchannel layers for given values of H_{c1} , H_{c2} and Ω are found through a very fast iterative procedure which uses previously computed dimensionless solutions of the parabolized Navier-Stokes equations in the entrance region of ducts having rectangular cross-sections with aspect ratios equal to those of the microchannels in the DL-MCHS. This preliminary solution is obtained using an in-house FEM code [13]. The microchannel heights corresponding to the selected values of the ratio H_{c2}/H_{c1} are listed in Table 2, while the microchannel inlet velocities in the two families of DL-MCHS are reported in Tables 3 and 4.

The coolant inlet temperature is $T_{in} = 300$ K. Since the temperature variations of the coolant (water) are expected to be small, the values of its thermophysical properties are assumed constant and evaluated at a temperature of 300 K: density $\rho = 995.6$ kg/m³, viscosity $\mu = 0.854 \times 10^{-3}$ kg/(m s), specific heat $c_p = 4180.6$ J/(kg K) and thermal conductivity $k = 0.610$ W/m K [14]. The thermal conductivity of silicon is $k_s = 148$ W/m K [11].

With the adopted values of velocity, the value of the Reynolds number based on the hydraulic diameter never exceeds 320 and, thus, the flow in the microchannels is laminar in all cases. Since the effects of body forces and viscous dissipation can be considered negligible, the conjugate

Table 2. Microchannel heights corresponding to different values of H_{c2}/H_{c1} in series #1 ($N_m = 54$, $W_c = 88\mu\text{m}$) and series #2 ($N_m = 64$, $W_c = 87\mu\text{m}$) of DL-MCHS

H_{c2}/H_{c1}	0	0.25	0.5	1	2	3	4	5	6
H_{c1} [μm]	1000	800	667	500	333	250	200	167	143
H_{c2} [μm]	0	200	333	500	667	750	800	833	857

Table 3. Microchannel velocities in series #1 of DL-MCHS for different values of Ω and $\Delta p_{c1} = \Delta p_{c2}$ (boldface: optimal geometry identified by Leng *et al.* [11]).

H_{c2}/H_{c1}	0	0.25	0.5	1	2	3	4	5	6	6.09
$\Omega = 0.0125$ W										
u_{c1} [m/s]	0.43	0.44	0.43	0.42	0.39	0.37	0.34	0.31	0.29	
u_{c2} [m/s]		0.34	0.39	0.42	0.43	0.44	0.44	0.44	0.44	
$\Omega = 0.05$ W										
u_{c1} [m/s]	0.86	0.87	0.86	0.83	0.78	0.73	0.68	0.63	0.58	0.57
u_{c2} [m/s]		0.68	0.68	0.83	0.86	0.86	0.87	0.87	0.87	0.87
$\Omega = 0.20$ W										
u_{c1} [m/s]	1.69	1.72	1.69	1.64	1.54	1.44	1.34	1.24	1.15	
u_{c2} [m/s]		1.24	1.54	1.64	1.69	1.71	1.72	1.72	1.73	

Table 4. Microchannel velocities in series #2 of DL-MCHS for different values of Ω and $\Delta p_{c1} = \Delta p_{c2}$ (boldface: optimal geometry identified by Leng *et al.* [11]).

H_{c2}/H_{c1}	0	0.25	0.5	1	2	2.12	3	4	5	6
$\Omega = 0.0125$ W										
u_{c1} [m/s]	0.39	0.40	0.39	0.38	0.36		0.34	0.31	0.29	0.27
u_{c2} [m/s]		0.31	0.36	0.38	0.39		0.40	0.40	0.40	0.40
$\Omega = 0.05$ W										
u_{c1} [m/s]	0.79	0.80	0.78	0.76	0.71	0.71	0.67	0.62	0.58	0.53
u_{c2} [m/s]		0.62	0.71	0.76	0.78	0.78	0.79	0.80	0.80	0.80
$\Omega = 0.20$ W										
u_{c1} [m/s]	1.55	1.57	1.55	1.50	1.41		1.32	1.23	1.14	1.06
u_{c2} [m/s]		1.23	1.41	1.50	1.55		1.57	1.57	1.58	1.58

convection-conduction heat transfer in the DL-MCHS is governed by the steady-state Navier-Stokes, continuity and energy equations

$$\rho \mathbf{v} \cdot \nabla \mathbf{v} = \mu \nabla^2 \mathbf{v} - \nabla p \quad (3)$$

$$\nabla \cdot \mathbf{v} = 0 \quad (4)$$

$$\rho c_p \mathbf{v} \cdot \nabla T = k \nabla^2 T \quad (5)$$

where \mathbf{v} is the velocity vector and p is the deviation from the hydrostatic pressure. Figure 1(b) shows a sketch of the cross-section of the computational domain, which corresponds to a repetitive portion of the DL-MCHS and is defined taking advantage of existing symmetries.

In this preliminary analysis, as in Ref. [11], we neglect the header effects on the inlet velocity distribution. Thus, appropriate boundary conditions are: uniform velocities u_{c1} and u_{c2} and uniform temperature T_{in} at microchannel inlets, pressure boundary conditions at outlets, symmetry conditions on symmetry planes, no-slip conditions at solid walls and uniform heat flux q''_w at the heated (bottom) wall, while all other sides are adiabatic. The numerical simulations are carried using the commercial code ANSYS Fluent 17.0, which is employed for the solution of the Navier-Stokes equations in the parts of the computational domain corresponding to the microchannels and of the energy equation in the whole domain, obviously, with $\mathbf{v} = 0$ and $k = k_s$ in the solid parts. The SIMPLE algorithm is selected to deal with the pressure-velocity coupling in the Navier-Stokes equations. The structured non-uniform computational grids, having finer spacing near the fluid-solid interfaces and the inlet/outlet boundaries, consist of a number of hexahedral cells ranging from 838 880 to 905 920 depending on the particular geometry. Based on preliminary grid independence tests, those grids have been deemed fine enough to yield grid independent results; in any event, they are much finer than those used by Leng *et al.* [11].

3. Computed results

The axial distributions of the bottom wall temperature T_w at the intersection with the microchannel vertical mid-plane are shown in Figure 2 for the two series of DL-MCHS and all the pumping powers. In the figure, the profiles shown by thick solid lines refer to the geometries and the optimal velocities of Leng *et al.* [11] reported in Table 1, while the profiles displayed using thick dashed lines are obtained using Leng's microchannel heights, but with velocities reported in Tables 3 and 4 that yield $\Delta p_{c1} = \Delta p_{c2}$. The thick dotted-dashed lines, instead, pertain to the single-layered MCHS. From Figs. 2(c) and 2(d), it is apparent that, with both series of DL-MCHS, there is degradation of the performance when velocities that yield equal pressure drop in both layers are adopted. However, one must keep in mind that this option allows a significant simplification of the piping and pumping systems. It also appears that, when the pressure drop is the same in both layers, the ratio H_{c2}/H_{c1} only has a marginal influence on $T_{w,max}$ and, thus, on R_T . Actually, for $\Omega = 0.0125$ W the $T_{w,max}$ yielded by the single-layered MCHS is lower than that obtained with any DL-MCHS and this is in agreement with what was found for low values of the flow rate by Wei *et al.* [6] and Xie *et al.* [7], who also analyzed single and/or parallel flow configurations. They explain this effect with the negative heat flux, i.e. heat flux from liquid to solid, occurring near the ends of the microchannels of a layer because of lower wall temperatures in those regions, which are effectively cooled by the low temperature fluid entering the microchannels of the other layer. The effect is reduced for larger values of the flow rate. The counter-flow configuration, however, always allows a better temperature uniformity of the heated surface, which is helpful in mitigating thermal stresses [7]. This positive effect is more relevant when $H_{c2}/H_{c1} > 1$. Similar conclusions can be reached by looking at Fig. 3, where maximum temperature differences $\Delta T_{w,max}$ and overall thermal resistances R_T of the two series of DL-MCHS are compared. The variations of R_T for different values of H_{c2}/H_{c1} are not larger than about 5% and in all cases the minimum of R_T is attained for $H_{c2}/H_{c1} = 2$. As far as the temperature uniformity is concerned, instead, it appears that when Ω increases the minimum value of $\Delta T_{w,max}$ is attained for larger values of H_{c2}/H_{c1} .

Finally, to illustrate the main features of the thermal field in a single and a double-layered MCHS of series #1, sample temperature maps on microchannel symmetry planes are shown in Fig. 4 for $\Omega = 0.05$ W. The positive effect of having two counter-flow streams on the temperature uniformity of the bottom surface is apparent. Figure 4 also confirms that, as already seen in Fig 3, the temperature variations on the heated surface are smaller for larger values of H_{c2}/H_{c1} .

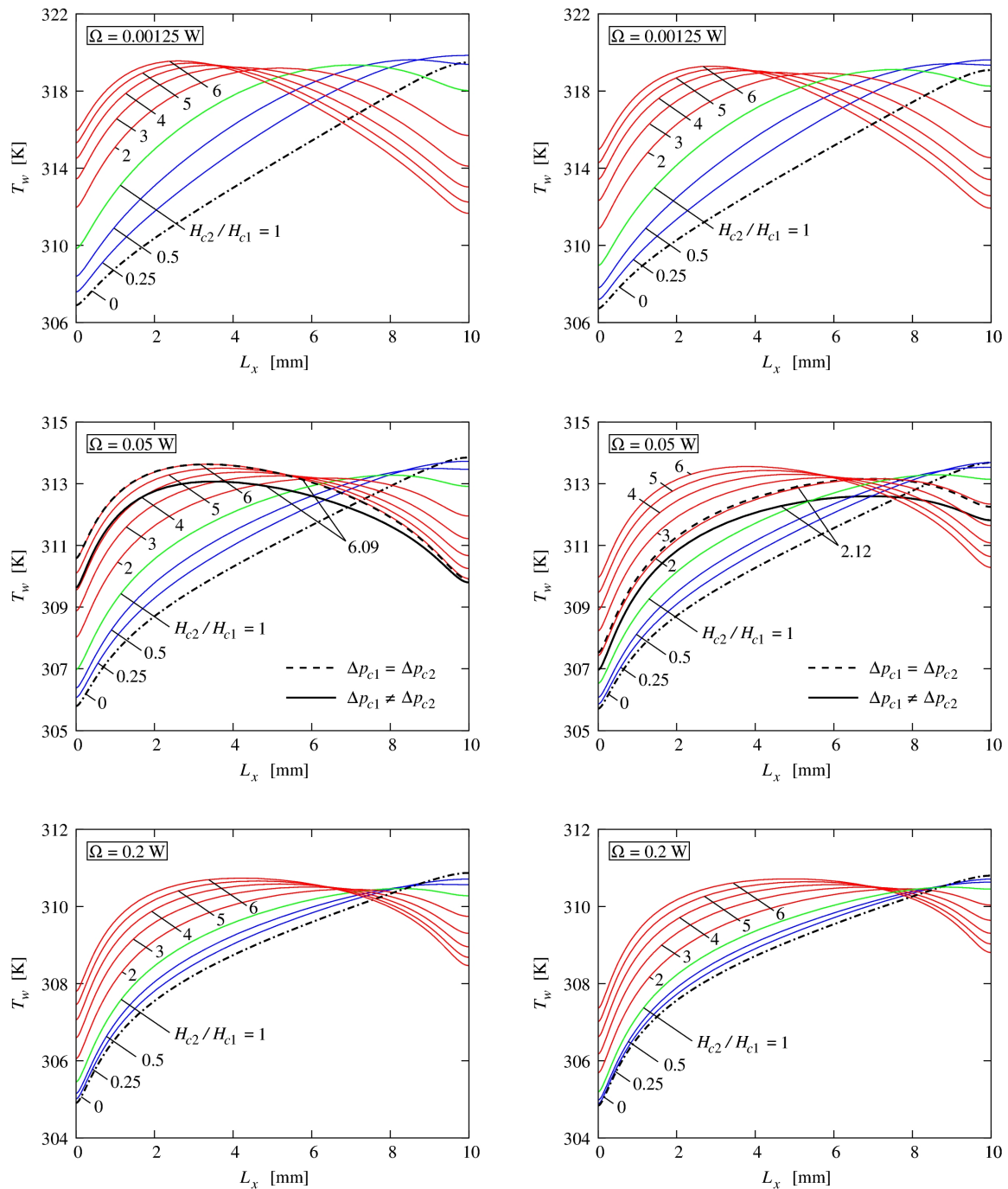


Figure 2. Axial temperature profiles on the bottom wall at the intersection with the microchannel vertical mid-plane: series #1 ($N_m = 54, W_c = 88 \mu\text{m}$) (left) and series #2 ($N_m = 64, W_c = 87 \mu\text{m}$) (right).

4. Conclusions

A parametric analysis has been carried out to investigate the thermal performance of DL-MCHS for different values of the relative channel height and fixed values of the total pumping power, with the additional constraint that the pressure drop be the same in the two layers in order to allow a much simpler header design, which can only include a single inlet and a single outlet. Single-layered MCHS have also been considered for additional comparisons. The main

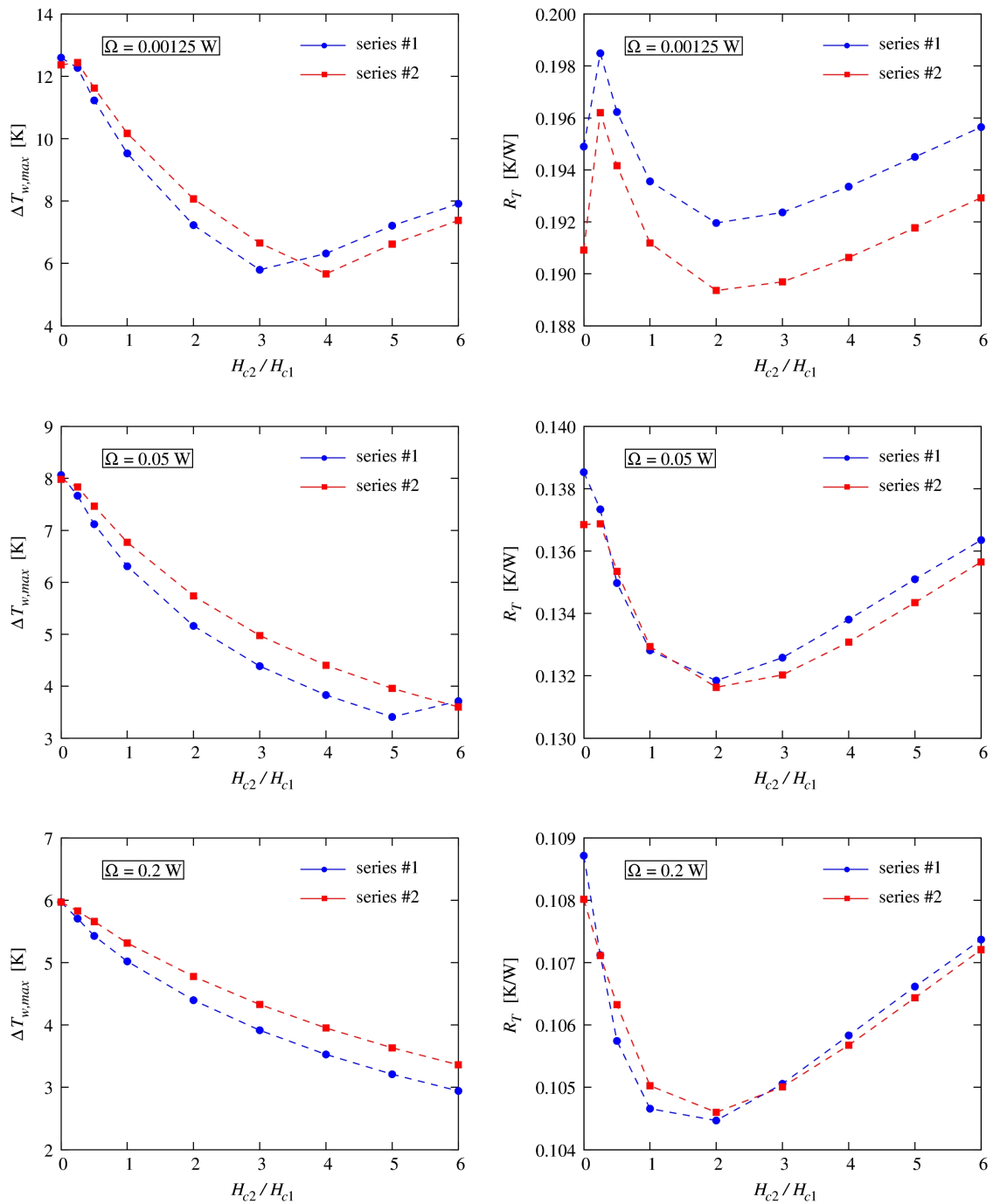


Figure 3. Comparisons of maximum temperature differences on the bottom wall $\Delta T_{w,max}$ (left) and overall thermal resistances R_T (right) of series #1 ($N_m = 54$, $W_c = 88\mu\text{m}$) and series #2 ($N_m = 64$, $W_c = 87\mu\text{m}$) of DL-MCHS.

conclusions are that, for fixed pumping power and equal pressure drop in the two layers of a DL-MCHS (i) the ratio of the heights of the upper and lower microchannels has a marginal effects on the overall thermal resistance but a significant influence on the temperature uniformity of the bottom (heated) surface and (ii) a better temperature uniformity is achieved when the heights of the upper microchannels are larger than those of the lower ones.

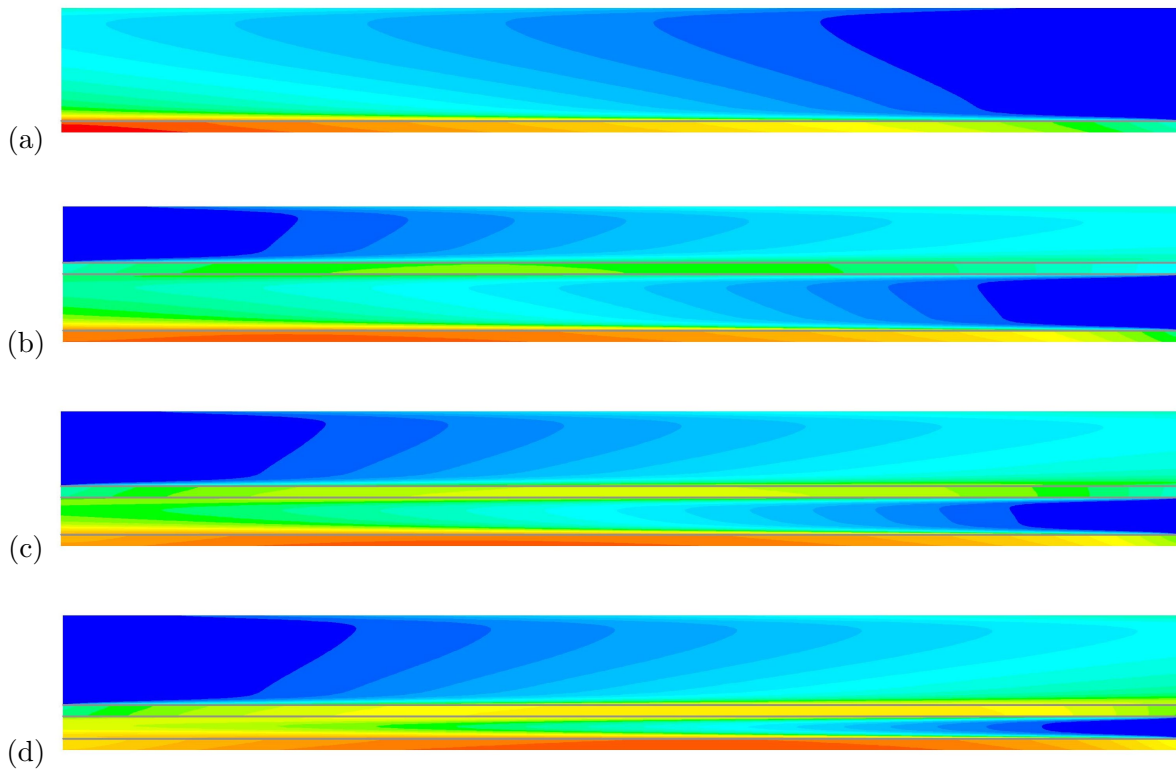


Figure 4. Temperature maps on microchannel symmetry planes in single and double-layered MCHS of series #1 for $\Omega = 0.05$ W: (a) $H_{c2}/H_{c1} = 0$, (b) $H_{c2}/H_{c1} = 1$, (c) $H_{c2}/H_{c1} = 2$ and (d) $H_{c2}/H_{c1} = 4$; (dark blue: 300 K, dark red: 314 K).

References

- [1] Qu W L and Mudawar I 2002 *Int. J. Heat Mass Transfer* **45** 2549–65.
- [2] Li, J and Peterson G P 2007 *Int. J. Heat Mass Transfer* **50** 2895–904.
- [3] Kou H S, Lee J J and Chen C W 2008 *Int. J. Heat Mass Transfer* **35** 577–82.
- [4] Wei X J and Joshi Y K 2003 *IEEE Trans. Compon. Packag. Technol.* **26** 55–61.
- [5] Saidi M H and Khiabani R H 2007 *ASME J. Heat Transfer* **129** 1230–36.
- [6] Wei X J, Joshi Y K and Patterson M K 2007 *ASME J. Heat Transfer* **129** 1432–44.
- [7] Xie G N, Liu Y, Sunden B. and Zhang W H 2013 *ASME J. Ther. Sci. Eng. Appl.* **5** 011004.
- [8] Lin L, Chen Y Y, Zhang X X and Wang X D 2014 *Int. J. Thermal Sciences* **78** 158–68.
- [9] Hung T C, Yan W M and Lei W P 2012 *Int. J. Heat Mass Transfer* **55** 3090–99.
- [10] Hung T C, Yan W M, Wang X D and Huang Y X 2012 *Int. J. Heat Mass Transfer* **55** 3262–72.
- [11] Leng C, Wang X D., Wang T H and Yan W M 2015 *Energy Convers. and Manage.* **93** 141–50.
- [12] Wu J M, Zhao J Y and Tseng K J 2014 *Energy Convers. and Manage.* **80** 550–60.
- [13] Nonino C, Savino S and Del Giudice S 2015 *Int. J. Numer. Methods Heat Fluid Flow* **25** 1322–39.
- [14] Lemmon E W, Huber M L and McLinden M O 2007 *NIST Standard Reference Database 23: reference fluid thermodynamic and transport properties-REFPROP* ver. 8.0 (National Institute of Standards and Technology: Gaithersburg, MD).